

GA-A24146

STATIONARY HIGH-PERFORMANCE DISCHARGES IN THE DIII-D TOKAMAK

by

**T.C. LUCE, M.R. WADE, J.R. FERRON, A.W. HYATT,
A.G. KELLMAN, J.E. KINSEY, R.J. LA HAYE, C.J. LASNIER,
M. MURAKAMI, P.A. POLITZER, and J.T. SCOVILLE**

NOVEMBER 2002

DISCLAIMER

This report was prepared as an account of work sponsored by an agency of the United States Government. Neither the United States Government nor any agency thereof, nor any of their employees, makes any warranty, express or implied, or assumes any legal liability or responsibility for the accuracy, completeness, or usefulness of any information, apparatus, product, or process disclosed, or represents that its use would not infringe privately owned rights. Reference herein to any specific commercial product, process, or service by trade name, trademark, manufacturer, or otherwise, does not necessarily constitute or imply its endorsement, recommendation, or favoring by the United States Government or any agency thereof. The views and opinions of authors expressed herein do not necessarily state or reflect those of the United States Government or any agency thereof.

STATIONARY HIGH-PERFORMANCE DISCHARGES IN THE DIII-D TOKAMAK

by

T.C. LUCE, M.R. WADE,* J.R. FERRON, A.W. HYATT,
A.G. KELLMAN, J.E. KINSEY,[†] R.J. LA HAYE, C.J. LASNIER,[‡]
M. MURAKAMI,* P.A. POLITZER, and J.T. SCOVILLE

This is a preprint of a paper to be submitted for publication in
Nucl. Fusion.

*Oak Ridge National Laboratory, Oak Ridge, Tennessee.

[†]Lehigh University, Bethlehem, Pennsylvania.

[‡]Lawrence Livermore National Laboratory, Livermore, California.

Work supported by
the U.S. Department of Energy under
Contract Nos. DE-AC03-99ER54463, DE-AC05-00OR22725,
W-7405-ENG-48, and Grant No. DE-FG02-ER54141

GENERAL ATOMICS PROJECT 30033
NOVEMBER 2002

ABSTRACT

Discharges which can satisfy the high gain goals of burning plasma experiments have been demonstrated in the DIII-D tokamak under stationary conditions at relatively low plasma current ($q_{95} > 4$). A figure of merit for fusion gain (β_{NH89}/q_{95}^2) has been maintained at values corresponding to $Q = 10$ operation in a burning plasma for >6 s or $36 \tau_E$ and $2\tau_R$. The key element is the relaxation of the current profile to a stationary state with $q_{min} > 1$. In the absence of sawteeth and fishbones, stable operation has been achieved up to the estimated no-wall β limit. Feedback control of the energy content and particle inventory allow reproducible, stationary operation. The particle inventory is controlled by gas fueling and active pumping; the wall plays only a small role in the particle balance. The reduced current lessens significantly the potential for structural damage in the event of a major disruption. In addition, the pulse length capability is greatly increased, which is essential for a technology testing phase of a burning plasma experiment where fluence (duty cycle) is important.

1. INTRODUCTION

The conventional design approach to a burning plasma in a tokamak yields a solution with high plasma current and an H-mode edge with edge localized modes (ELMs). This strategy has been extensively documented in the ITER Physics Basis [1]. Because the pressure limit, the density limit, and the energy confinement all scale linearly with plasma current using the conventional design rules, the fusion power and gain increase with plasma current. The principal constraint on the magnitude of the plasma current is the risk of a major disruption, i.e., a sudden, complete termination of the plasma current. The potential for damage to the mechanical structure of the tokamak by means of induced electromagnetic forces and to the plasma-facing components due to a rapid deposition of the magnetic and thermal stored energy in the plasma is significant. The compromise between the increase in fusion performance and the potential for damage as the plasma current is increased is typically struck at $q_{95} \approx 3$, where q_{95} is the “safety factor” at the flux surface with 95% of the poloidal flux at the boundary. For a given magnetic geometry, the safety factor is proportional to the ratio of the toroidal magnetic field (B) to the plasma current (I_p).

Discharges developed in the DIII-D tokamak offer an alternate compromise solution which would achieve many of the performance goals of ITER or other burning plasma experiments. These discharges project to similar fusion gain (Q) as the present baseline scenario at lower plasma current for the same device size and toroidal magnetic field. The lower plasma current both reduces the potential for damage in the case of disruption and lengthens the possible discharge duration through reduced flux consumption and higher bootstrap current fraction. These discharges have been operated in the DIII-D tokamak under stationary conditions where the pressure profile, the current profile, and the wall particle balance are all in equilibrium. The discharges have only ~50% noninductive current so they are not a true steady state. The divertor tiles in DIII-D are not actively cooled; therefore, heating of the divertor strike points could also be a limiting factor in DIII-D, although not a fundamental limit in future devices. At present, the limitations on discharge duration in DIII-D have been conservative settings of the protection hardware on power supplies, not physics limits. It appears that the true limit on DIII-D pulse length in this mode of operation will be the maximum energy which can be input by the auxiliary heating systems.

The technique by which these discharges are formed and maintained will be discussed in the following section. The details of the current profile evolution, limits of stability, particle balance and divertor issues, and transport will then be addressed. Finally, the key

issues which need to be addressed for projection to a burning plasma experiment will be discussed, followed by summary and conclusions.

2. DEVELOPMENT OF STATIONARY DISCHARGES IN DIII-D

The realization of a stationary pressure profile, current profile, and wall inventory in DIII-D requires several important control and discharge design elements. The key element to stationary discharges at high Q conditions is an equilibrated current profile that is stable to sawteeth and fishbones. This allows access to much higher β . For the pressure profile, the energy content is held stationary by feedback control of the neutral beam injection power. The fuel and impurity densities must also be constant. The fuel density control is achieved by active pumping and gas puffing. The impurity sources are controlled essentially by effective divertor design. Finally, limiting the wall particle inventory is important not only to the dynamics of the fuel density but also to demonstrating that the high performance conditions are not due to transient wall conditions. The feedback control of the energy and particle content of the plasma throughout the discharge yield not only stationary conditions, but also excellent reproducibility of these conditions.

A representative discharge of this type is shown in Fig. 1. The discharge is formed on the inside wall and then diverted at 300 ms to form a double-null plasma. The magnetic geometry is biased vertically upward so that the top null is dominant. This has the desired effect of increasing the power required to induce an H-mode transition and also engages the upper cryopumps to allow control of the particle inventory in the H-mode phase. (See Section 5 for further details of the particle control.) The radial distance between the field lines connecting the upper and lower nulls measured at the outer midplane (dR_{sep}) is +1.0–1.5 cm during the current ramp up. (The sign convention is such that $dR_{sep} > 0$ means the upper null is dominant.) Two neutral beams ($P_{NBI} = 4.8$ MW) are injected at 300 ms to slow the evolution of the plasma current density. The q profile [Fig. 2] is monotonic at these early times, but nearly flat inside of $\rho = 0.6$. (The normalized radius ρ

is the square root of the enclosed toroidal flux normalized to the value within the last closed flux surface.) Two more neutral beams at 1/3 duty cycle are started (out of phase) at 800 ms to further slow the current evolution. The current profile at the end of the current ramp is hollow yielding a q profile with a minimum near $\rho = 0.6$.

The two important elements of the current ramp phase are maintaining an L-mode edge and controlling the wall particle inventory by pumping. If the plasma transitions to an H-mode edge during the current ramp up, the edge is so hot that the current cannot penetrate and the internal inductance (ℓ_i) drops. The achievable β (the ratio of the kinetic to the magnetic energy density) in discharges with monotonic q profiles in DIII-D is found to be proportional to ℓ_i [2], so maximizing ℓ_i is important to achieving high performance. The end of the current ramp up and a programmed reduction of dR_{sep} to 0.6 cm lower the power required to make a transition to H-mode. The two modulated neutral beam injectors are switched from 1/3 to 2/3 duty cycle at 1100 ms. These actions result in a reproducible L-H transition at 1200 ms. The target density has been adjusted empirically to give a short ELM-free period, so that the density in the H-mode phase does not overshoot the desired value. The density during the current ramp up and P_{NBI} are correlated strongly with the resultant q profile since the current profile evolution is dominated by the resistivity.

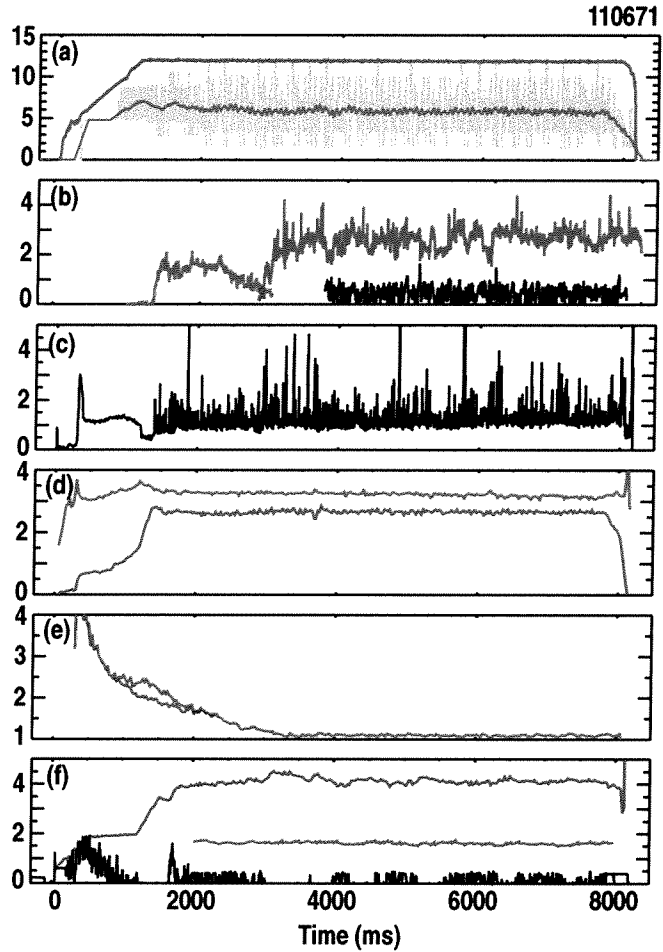


Fig. 1. Time histories of various plasma parameters for a typical long-pulse stationary discharge ($B = 1.7$ T). (a) (red) $10\times$ Plasma current I_p (MA), (grey) neutral beam power P_{NB} (MW), (magenta) P_{NB} with a 200 ms moving average (MW), (b) magnetic perturbations measured at the vacuum vessel for $n=3$ (green), $n=2$ (red), and $n=1$ (blue) (G), (c) D_α emission from the upper divertor (10^{15} photons/cm²/s), (d) β_N (red) and $4\ell_i$ (green), (e) q_{min} (red) and $q(0)$, (f) (red) line-averaged density \bar{n}_e (10^{19} m³), (green) Z_{eff} from carbon, (black) gas flow $\Phi_D/100$ (not including neutral beam sources) (torr· ℓ /s).

The discharge makes a smooth transition from an ELM-free phase to a steadily ELMing edge [Fig. 1(c)]. The ELMs are presumably Type I, due to their size and the resultant good global confinement. The ELMs provide both density and impurity regulation in the stationary phase [Fig. 1(f)]. The density does not overshoot the target value of $4 \times 10^{19} \text{ m}^{-3}$. The Z_{eff} , determined from active charge exchange spectroscopy assuming carbon as the sole impurity, is about 1.6 in the core and is not increasing. Carbon is expected to be the dominant impurity and no significant metallic impurities are observed. The density is under feedback control using gas puffing and active pumping.

The plasma energy content is also under feedback control [Fig. 1(d)]. The neutral beam injectors are controlled [Fig. 1(a)] to maintain a constant predetermined level of diamagnetic flux. The requested energy corresponds to a normalized β (β_N) of 2.7, which is about 85% of the expected no-wall β limit for these discharges as estimated by $4\ell_i$ [Fig. 1(d)]. (The normalized β is defined as $\beta/(I/aB)$. The β_N quoted in this paper will be in units %-MA/m·T.) A low level of magnetic fluctuations is seen throughout the stationary phase of the discharge [Fig. 1(b)]. From the end of the ELM-free period to ~ 3000 ms, a $n=3$ oscillation is observed. From 2000 ms, the mode frequency, the measured plasma rotation, and the q profile are consistent with the existence of a tearing mode at the $5/3$ surface. Prior to this, the oscillations may be a $7/3$ tearing mode, but the correlation among the measurements is not so good. No poloidal distributed magnetic measurements or radially-resolved electron temperature fluctuation measurements from electron cyclotron emission (ECE) are available at this time. After 3000 ms, the dominant mode is a $3/2$ tearing mode. Note that the maximum mode amplitude at the wall is ~ 3 G, which corresponds to an island with ~ 4 cm half-width in the plasma. It is important to note that the current profile relaxes to a stationary value with $q_{\text{min}} = q(0) \sim 1$, yet no sawtooth or fishbone activity is measured. There is, however, a small (< 1 G) $n=1$ mode with a rotation frequency corresponding to a location near the axis. The magnetics data show no rapid transients except those associated with the ELMs.

Determination of the mode numbers given in the preceding relies heavily on the correlation of the measured toroidal rotation, the observed mode frequency, and the reconstructed $q(0)$ profile (including MSE data). The toroidal mode number is given quite reliably by measuring the phase difference between two magnetic probes with known

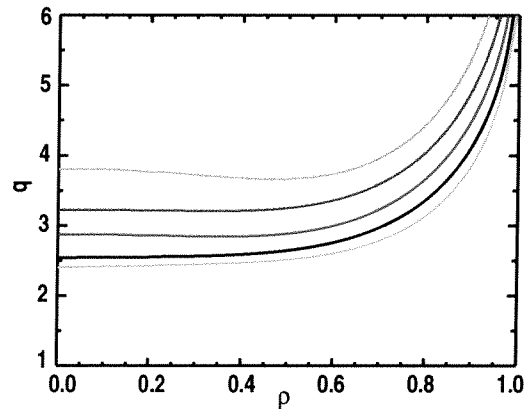


Fig. 2. Reconstructed q profile using MSE and magnetics data versus normalized radius. The profiles are shown at 100 ms intervals starting at 500 ms (upper trace).

spacing toroidally. This can be verified by either phase analysis or singular value decomposition of the entire toroidal array [3]. In cases where the full poloidal magnetic probe array is available, the poloidal mode number (m) can also be estimated. For the discharge shown in Fig. 1, the poloidal data is available from 4000–4600 ms. The mode is clearly an $m=3/n=2$ mode [Fig. 3(a)] with a rotation frequency of 38 kHz [Fig. 3(c)]. The location of the $q = 1.5$ surface ($\rho = 0.45$) corresponds to a measured rotation of 16 kHz. The mode rotation is consistent with a modest propagation of the mode (in the plasma frame) in the ion diamagnetic direction ($f_{\text{mode}}/n = 19$ kHz vs. 16 kHz plasma rotation) as observed in other DIII-D experiments [4]. The $n=3$ mode after 2000 ms is consistent with a $m=5/n=3$ mode (Fig. 4). Note that the flat spot in the rotation corresponds to the location of the minimum in q and $q_{\text{min}} \sim 5/3$. The poloidal mode number identification is fairly certain in this case since there is little chance that a $q = 4/3$ surface exists and the $q = 7/3$ surface corresponds to a much lower rotation frequency.

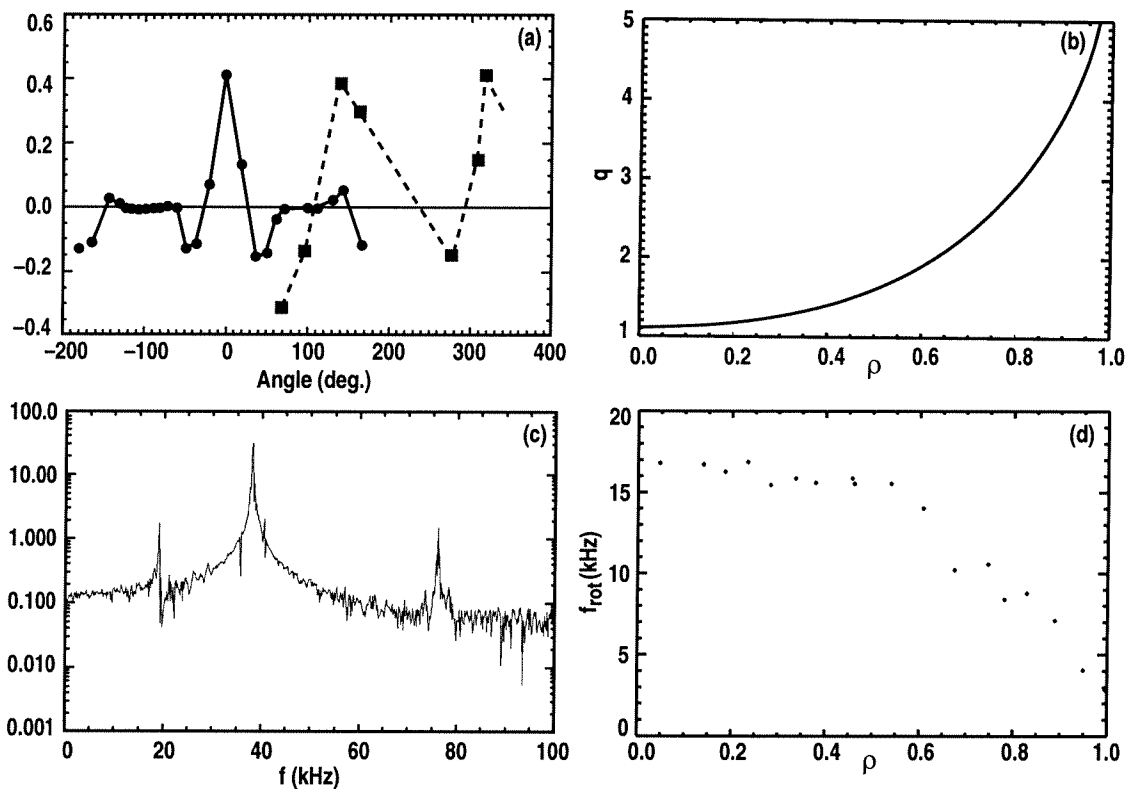


Fig. 3. Signals for identification of the $m=3/n=2$ mode at 4500 ms in the discharge shown in Fig. 1. The identification is explained in the text. (a) Spatial eigenfunction of the largest eigenmode from a simultaneous singular value decomposition (SVD) of the poloidal and toroidal magnetic data (dB/dt). The poloidal data is plotted versus poloidal angle of the magnetic probe with $\theta = 0$ at the outside midplane and positive angles are above the midplane. The toroidal magnetic data are plotted versus toroidal angle (the reference is arbitrary). (b) Reconstructed q profile versus normalized radius ρ . (c) Fourier transform of the temporal eigenfunction of the largest SVD eigenmode versus frequency. (d) Measured toroidal rotation from charge exchange recombination (CER) spectroscopy of carbon versus normalized radius ρ .

As discussed in detail in subsequent sections, these discharges are in equilibrium with respect to the pressure profile, the current profile, and the wall particle inventory. The pressure profile remains constant for ~ 36 global energy confinement times (τ_E) while the current profile is stationary for ~ 2 current redistribution times (τ_R). This stationary phase is all the more remarkable because of the high level of performance achieved. As mentioned above, $\beta_N = 2.7$ or $\sim 85\%$ of the expected no-wall β limit. The confinement time compared to the ITER-89P scaling [5] is 2.5. This gives a normalized performance product $\beta_N H_{89} = 6.8$ at $q_{95} = 4.2$. A common figure of merit for fusion gain is $\beta_N H_{89} / q_{95}^2$. In this discharge the value of $\beta_N H_{89} / q_{95}^2$ achieved in steady conditions is 0.39. For reference, the present ITER-FEAT reference scenario [6] has the possibility of $Q = 10$ operation at $\beta_N = 1.8$, $H_{89} = 2.1$, and $q_{95} = 3.0$, giving $\beta_N H_{89} / q_{95}^2 = 0.42$. Since the fusion gain would be comparable at 30% lower current (with corresponding reductions in the impact of a major disruption and increase in pulse duration), the discharges discussed here clearly warrant further investigation as an alternative (or preliminary) means to achieve the fusion gain objectives in a burning plasma experiment.

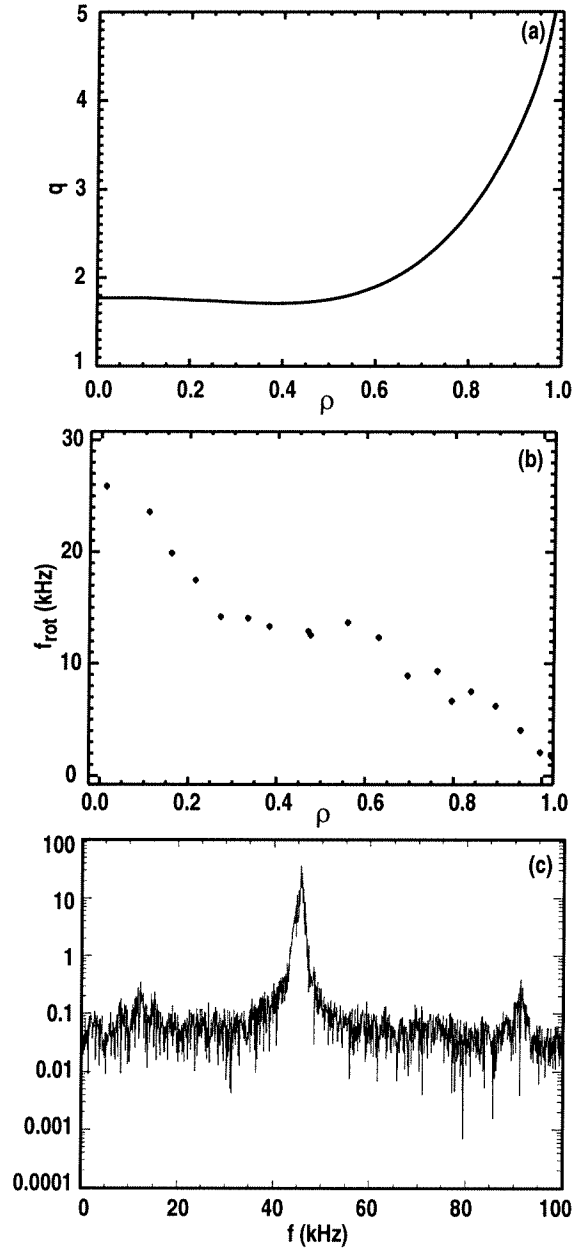


Fig. 4. Signals for identification of the $m=5/n=3$ mode at 2100 ms in the discharge shown in Fig. 1. (a) Reconstructed q profile versus normalized radius ρ . There is a shallow minimum near $\rho = 0.4$ at $q = 5/3$. (b) Fourier transform of the magnetic signal versus frequency (kHz). (c) Measured toroidal rotation from CER spectroscopy of carbon versus normalized radius ρ .

3. EVOLUTION OF THE CURRENT DENSITY PROFILE

A direct method to show that the current profile has become stationary is to examine the time histories of the magnetic pitch angles measured inside the plasma by motional Stark effect (MSE) spectroscopy [7]. The data from the tangential viewing array are shown in Fig. 5. From ~4000 ms until the neutral beam power drops at 7800 ms, the measured pitch angles are constant within the measurement uncertainties. The lack of time evolution of the pitch angle implies that $\partial B_z/\partial t = 0$ for the DIII-D geometry, which indicates the electric field is constant from $R = 1.5$ –2.1 m. Other MSE views indicate the electric field is constant out to the radius where the ELMs have a substantial effect and even there the field is constant in a time-average sense.

The time scale on which the current profile equilibrates is consistent with estimates of the redistribution time using neoclassical resistivity. This redistribution time is defined here as the time for the lowest radial moment of the profile to decay [8] with the constraint of constant total current. The characteristic time is evaluated using neoclassical conductivity [9] and the real plasma cross-sectional area. For the discharge shown in Figs. 1 and 5, $\tau_R = 2$ s. The reconstructed current profiles, which use magnetics and MSE data, (Fig. 6) show that by 3450 ms the current density reaches a peaked profile which is similar to the profile at 7450 ms. This validates τ_R as characteristic of the relaxation time scale of the current.

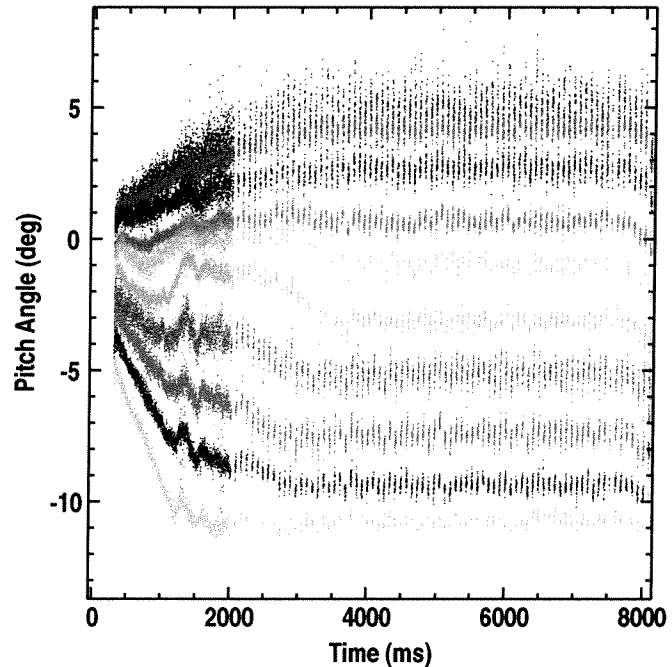


Fig. 5. Time history of magnetic pitch angles (deg) from the discharge shown in Fig. 1 measured by the tangential viewing MSE system ($R = 1.5$ –2.1 m). Each color represents a separate channel. The probe beam is run continuously until 2000 ms, then modulated to allow measurements throughout the discharge.

Using this same resistivity model and the associated bootstrap current, together with the neutral beam current drive calculation, the expected equilibrium current profile can be calculated. The resultant profile has $q_{\min} < 1$. No high-frequency magnetic perturbations

are detected which would indicate a significant redistribution of the fast ion population and a corresponding broadening of the neutral beam current drive. Analysis of the internal loop voltage [10] indicates a voltage source at the location of the 3/2 tearing mode [11]. It is speculated that this small voltage source at $\rho = 0.5$ is sufficient to broaden the current profile to allow q_{\min} to remain above 1. In the absence of some unknown mechanism for a stationary island to generate an axisymmetric voltage, it would appear that the fluctuations in the amplitude, seen in Fig. 1(b), have to play an essential role. Because of the non-diffusive current profile

evolution in the vicinity of the tearing mode and the uncertainty in the average effect of the ELMs on the edge bootstrap current, a definitive identification of the key elements to avoidance of sawteeth and fishbones has not yet been obtained.

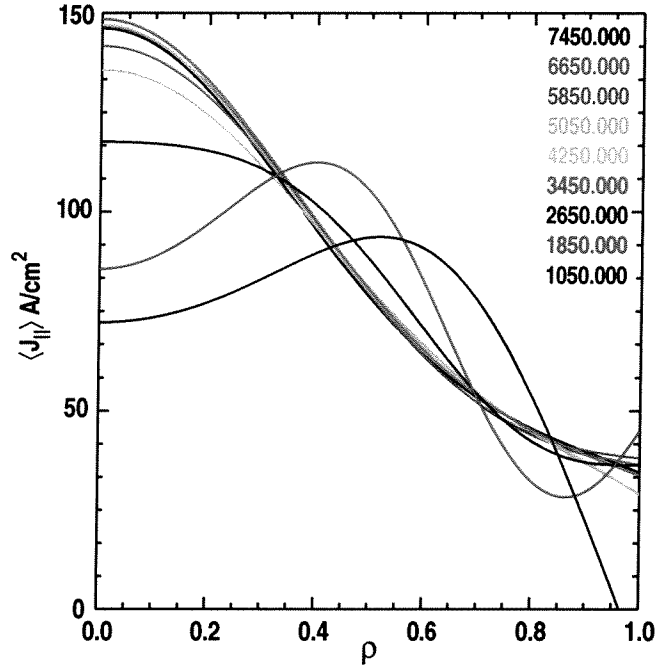


Fig. 6. Radial profiles of the reconstructed flux-surface-averaged current density $\langle J_{\parallel} \rangle$ of the discharge shown in Fig. 1 at 800 ms intervals (corresponding to measurement times of the MSE data later in the discharge).

4. STABILITY

Even though the plasma is clearly unstable to $n=3$ and, later, $n=2$ tearing modes, these do not present a limit to the attainable plasma pressure. Initial studies [12] found that the 2/1 tearing mode did represent a definite pressure limit. If the requested β was increased from the outset of the feedback controlled phase, the attainable β_N was limited to <2.9 . Since P_{NB} was under feedback control, all of the available power was applied as the 2/1 mode caused the β to drop, yet this was insufficient to maintain the requested β . This β limit is typically not a disruptive limit, although the full beam torque probably prevents the mode from locking to the wall, which is the normal prerequisite to a disruption.

Subsequent experiments have demonstrated that significantly higher β operation is possible, up to the expected no-wall limit ($4\ell_i$), if the increase in β occurs after the current has reached its stationary state. An example of a step increase in β is shown in Fig. 7. The requested β_N is raised to 3.2 and held for 600 ms until a power supply fault initiates a shutdown of the discharge. The energy confinement also improves ($H_{89} = 2.8$) giving $\beta_{NH_{89}} = 8.9$ and $\beta_{NH_{89}}/q_{95}^2 = 0.44$. If the requested β_N is raised further, to well above $4\ell_i$, a 2/1 tearing mode reliably appears. This is consistent with recent theoretical studies which indicate the classical tearing stability index Δ' can become positive as an ideal magnetohydrodynamic (MHD) limit is approached [13], leading to a tearing mode.

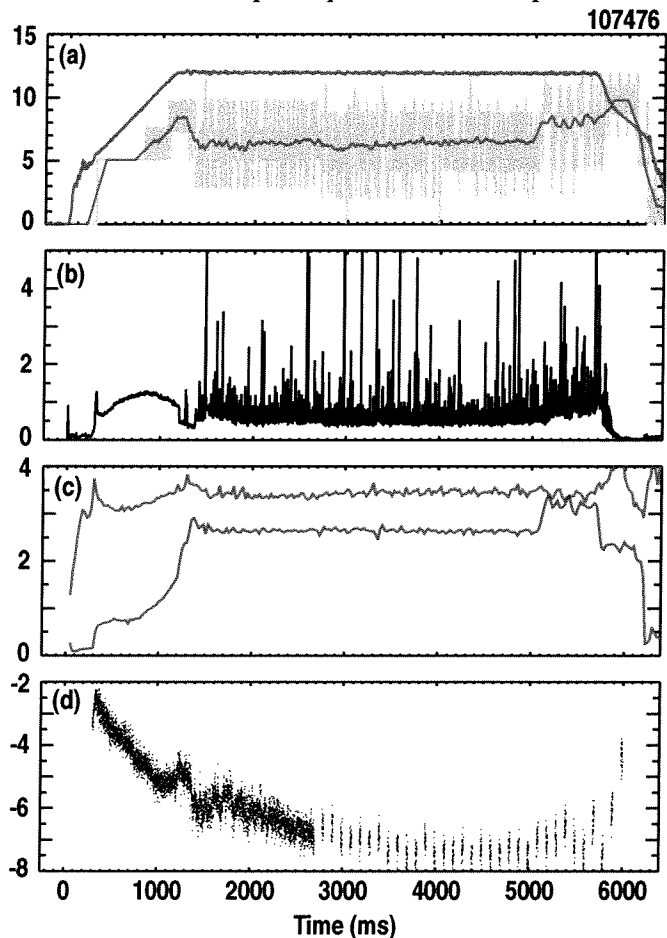


Fig. 7. Time histories of various plasma parameters for a case where the requested β has a step increase to $\beta_N = 3.2$ at 5000 ms ($B = 1.7$ T). (a) (red) $10\times$ Plasma current I_p (MA), (grey) P_{NB} (MW), and (magenta) P_{NB} with a 200 ms moving average (MW), (b) upper divertor D_α (10^{15} photon/cm²/s), (c) (red) β_N and $4\ell_i$ (green), (d) magnetic pitch angle measured by MSE (γ_{MSE}) at $R = 1.93$ m.

The β can also be raised gradually as shown in Fig. 8. Once the current profile has been established, the β request was smoothly increased starting at 2300 ms up to $\beta_N = 3.2$ at 5400 ms and held there. This was the maximum available neutral injection power at the time of the discharge. The β_N corresponds to the expected no-wall β limit, as estimated by $4 \ell_i$. From the MSE measurement [Fig. 8(d)], there is little change in the current profile with the increased β_N .

Enhanced stability to tearing modes in the absence of sawteeth has been observed previously in DIII-D [14]. The current profile in those cases was transiently maintained with $q_{\min} > 1$, but eventually relaxed to a sawtooth-ing plasma. In that case, no tearing modes were destabilized until the approximate no-wall limit was reached, as in the present case. In comparison to the original discharges in [12], the discharges in Figs. 7 and 8 have about 10% higher density. Since the temperatures are also slightly higher, it is unlikely that the improved stability is due to higher collisionality, which is inferred to be stabilizing from database scaling studies [15]. Evidently, the improved stability is due to subtleties in the current profile which modify either Δ' or the ideal limit. A fiducial discharge with similar shape and field operated with $q_{95} = 3.1$ was unstable to the 2/1 tearing mode at $\beta_N = 2.8$. The mode locked and disrupted the plasma. This is consistent with the previous DIII-D experience [14] and the ITER design rules which recommend limiting β_N well below 2.5 to avoid the tearing modes.

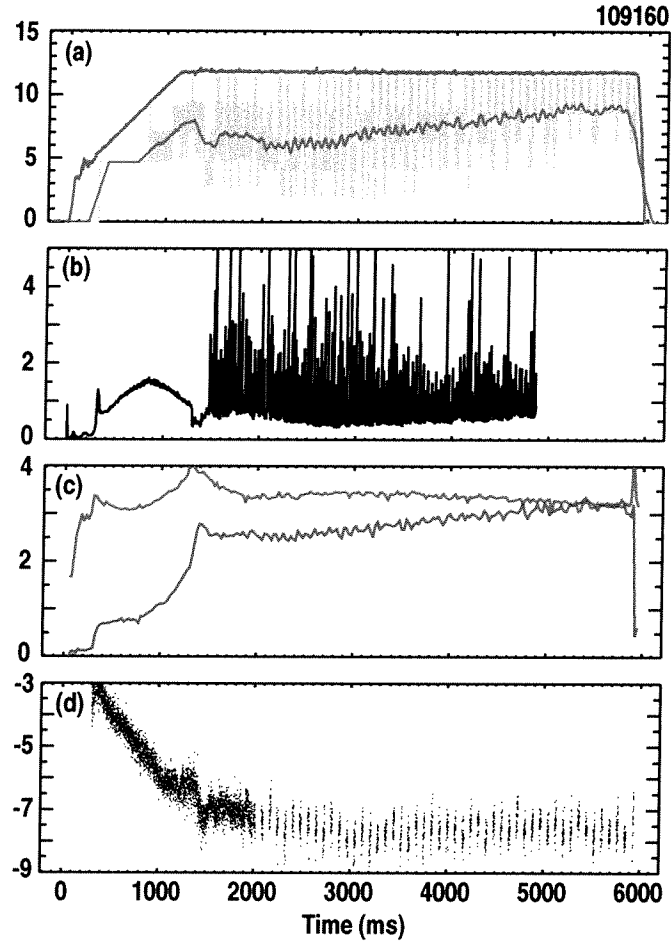


Fig. 8. Time histories of various plasma parameters for a case where the requested β is slowly ramped to $\beta_N = 3.2$ at 5000 ms ($B = 1.7$ T). (a) (red) $10\times$ Plasma current I_p (MA), (grey) P_{NB} (MW), and (magenta) P_{NB} with a 200 ms moving average (MW), (b) upper divertor D_α (10^{15} photon/cm²/s), (c) (red) β_N and (green) $4 \ell_i$, (d) magnetic pitch angle measured by MSE (γ_{MSE}) at $R = 1.93$ m.

5. WALL INTERACTIONS

In these discharges, the wall plays little role in the particle balance during the stationary phase. The various components of the particle balance are shown in Fig. 9. Details of how the particle balance during a discharge is determined can be found in Ref. [16]. It is clear from the small variation in the wall inventory after the L-H transition at 1200 ms [Fig. 9(c)], that the wall plays an insignificant role in the particle balance. The wall is very slowly returning the particles it accumulated during the L-mode current ramp up. This indicates that the control obtained over the particle inventory in the plasma is maintained by active feedback and pumping rather than preconditioning of the walls. Previously reported discharges showed almost no change in the wall inventory over the 5 s stationary phase [11].

To control the particle inventory effectively after the L-H transition, it is necessary to limit the amount of gas which goes to the wall during the current ramp up phase [17]. This is consistent with the particle balance shown in Fig. 9. The wall at early times is more effective than the pumps at retaining the particles which are not taken

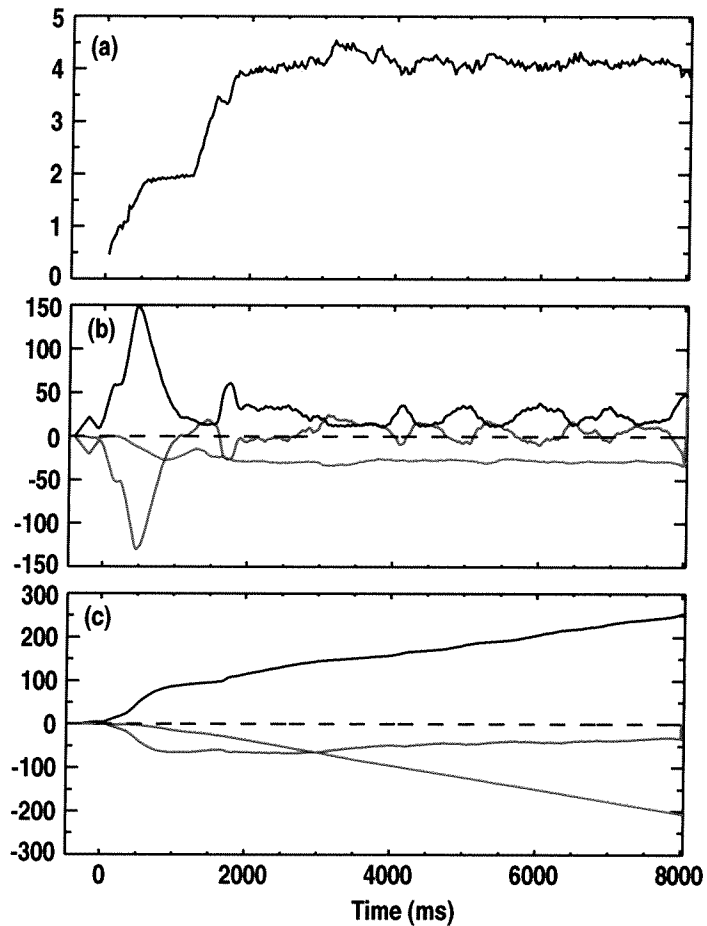


Fig. 9. Time histories of quantities relevant to the particle balance for the discharge shown in Fig. 1. (a) Line-averaged density (10^{19} m^{-3}), (b) total gas injection and NB injection rates (black) ($\text{torr}\cdot\ell/\text{s}$), total removal rates for the inner and outer divertor cryopumps (green) ($\text{torr}\cdot\ell/\text{s}$) and wall rate (red) ($\text{torr}\cdot\ell/\text{s}$). The sign convention is that positive rates indicate a source of particles to the plasma. (c) Integrated sources ($\text{torr}\cdot\ell$) from the gas injectors and neutral beams (black), divertor cryopumps (green), and the wall (red).

up by the plasma. If the cryo-pumps were not effectively coupled to the plasma during the early phase, the density rise at the L-H transition would overshoot the target density [17]. Helium glow cleaning is carried out between discharges, but the primary effect of the glow cleaning for plasma operations with effective cryopumping is to regenerate the cryopumps and remove any volatile impurities.

The divertor tiles in DIII-D are not actively cooled, so the temperature on the tile surfaces rises continuously throughout the discharge. The tile material is ADJ Graphite and is expected to undergo sublimation around 2000°C. In previous long-pulse discharges, the strike points in the divertor were held fixed for maximum pumping. With ~48 MJ energy input, the tile center were measured to reach 1150°C (Fig. 10) with tile edges 200°–300°C higher. The effect of toroidal asymmetry is unknown since the infrared camera measurements are made at only one toroidal location. Despite temperatures reaching levels near the predicted threshold for radiation-induced sublimation, no enhancement of carbon is measured in the core [Fig. 1(f)]. Significant erosion and redeposition of carbon in the upper divertor was observed upon entry to the tokamak after these discharges. While it is not possible to attribute these effects solely to the long-pulse experiments, it is indicative that the divertor is performing well in its two main functions — to provide control of the hydrogenic particle inventory and to isolate the plasma from impurity sources where the field lines cross a material surface. In preparation for even higher energy input during a single discharge, the outer divertor strike point was programmed to oscillate at ~1 Hz over a distance of ~1.5 cm in the discharge shown in Fig. 1, clearly reducing the average rate of temperature rise on the tile centers (Fig. 10).

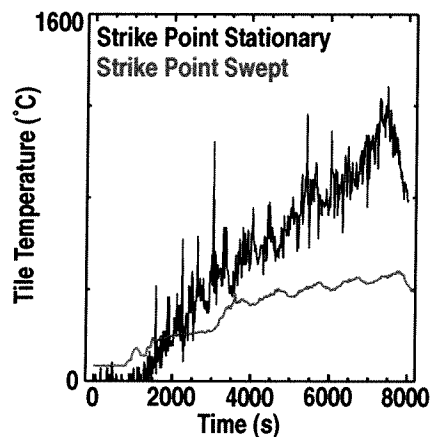


Fig. 10. Time histories of the tile temperatures measured by infrared camera for a discharge with stationary (black) and oscillating (red) outer divertor strike point locations.

6. ENERGY CONFINEMENT

The energy confinement in these discharges compared to the ITER-89P scaling relation [5] improves with increasing β_N . This is consistent with the observation that most scaling relations determined from multi-machine databases have a significant degradation in confinement with increasing β , while dedicated experiments do not see this degradation [18,19]. This inconsistency between the design rules and the experiment leads to design optimizations at lower β . When the assumed β limit due to tearing modes is low ($\beta_N \sim 2.0$), this does not have a significant impact on the design. However, in situations where higher β_N is readily achievable (up to $\beta_N = 3.2$ in the present case), severe degradation with β in scalings such as ITER-93H [20] lead to performance limited by device parameters rather than the β limit [21].

It may be surprising that confinement enhancement of up to $H_{89} = 2.8$ can be obtained with a saturated 3/2 tearing mode. However, estimates of the reduction in stored energy, which assume complete flattening of the pressure profile across the island [22], indicate <10% reduction in τ_E is expected. Estimates of the island width from the magnetics are used. In the case of the discharge shown in Fig. 1, the inferred island half-width is only 4 cm. These estimates of the confinement reduction are confirmed in discharges where the tearing mode onset is late. This allows comparison of the power demanded by the feedback system to maintain constant β in the periods with and without the tearing mode. The increase in the power demand is <10% after the mode is observed.

The energy confinement observed is also consistent with estimates of the transport driven by drift-wave turbulence. Figure 11 shows that the profiles calculated using the GLF23 model [23] compare well with the measured electron and ion temperature profiles. The GLF23 model incorporates turbulent transport from ion temperature gradient modes, trapped electron modes, and electron temperature gradient modes including the effects of $E \times B$ shear stabilization of long wavelength modes. The measured density, rotation, impurity density, and radiation loss are taken as input, as is the deposited neutral beam power density. The electron-ion exchange is evaluated self-consistently through the time evolving calculation. The boundary condition of the calculation is specified at $\rho = 0.85$, outside of which other effects not included in the model may contribute significantly to the transport. The value is adjusted slightly from the experimental value to maximize the range over which the model agrees with the data. The $E \times B$ shear has a modest effect in these calculations in that the transport is reduced from the transport calculated in the absence of $E \times B$ shear; however, the effective diffusivity remains well above the neoclassical level, indicating the $E \times B$ shear does not

fully stabilize the turbulence. The main conclusion of this comparison is that the high confinement compared to multi-machine scalings observed in these discharges does not require an extraordinary means of enhanced confinement beyond that predicted by a standard models.

7. PROSPECTS AND OUTSTANDING ISSUES FOR EXTRAPOLATION TO BURNING PLASMA EXPERIMENTS

The range over which the density, magnetic field, and plasma current of this type of discharge have been varied is fairly small at present. However, this has been by design; in no instance was the variation limited due to the loss of the performance. Still, the previous sections indicate a substantial amount of understanding has been gained.

The key element from which all of the positive aspects seem to flow is the stationary current profile with $q_{min} > 1$. The present understanding indicates that the small tearing mode at the $q = 1.5$ surface plays an essential role in the final state achieved. Without a physics model for the apparent dynamo action, which appears as an axisymmetric voltage source, it is unclear how this will extrapolate to any other device. Experiments are needed with counter fast wave current drive on-axis or co-ECCD off-axis to see if such current profiles can be maintained without the tearing mode.

The enhanced stability appears to follow directly from the avoidance of sawteeth or equivalently maintaining $q_{min} > 1$. To increase further the fusion power, lower q_{95} operation would be desirable. However, the restriction of $q_{min} > 1$ will likely limit how far q_{95} can be reduced in this mode of operation without noninductive current drive. Discharges of this type have been operated in the range $q_{95} = 3.9-4.5$. Replacement of neutral beam injection with fast wave or electron cyclotron heating may facilitate operation at lower q_{95} due to the reduction in central current drive. (At present, all neutral beams are co-injection on DIII-D with corresponding central co-current drive.) A broad profile of co-current drive with ECCD may also extend the operating space by altering Δ' and the no-wall β limit.

In principle, it may be possible to extend operations into the region between the no-wall β limit and the ideal-wall β limit. These discharges are rotating sufficiently fast that the DIII-D wall should provide significant stabilization. No indication of a resistive wall mode has been found as β is increased. In every case, the β has been limited by the onset of a 2/1 tearing mode when the β rises above the estimated no-wall β limit. Recent experiments using this type of discharge have successfully demonstrated complete suppression of the 2/1 tearing mode at low β . No attempt has been made to increase β during suppression. While the prospects for operating above the DIII-D no-wall limit are

unknown at this point, it is important to recall that levels of performance corresponding to $Q = 10$ in ITER-FEAT have been maintained in DIII-D without going above the no-wall limit.

The main question with respect to extrapolation of the confinement to a burning plasma is the role of T_i/T_e in achieving good confinement. As shown in Fig. 11, T_i/T_e is everywhere >1 , which has been shown to be favorable for confinement [24] and is expected to be stabilizing to drift-wave turbulence. Limited scans of density in DIII-D indicate that the reduction of confinement as $T_i/T_e \rightarrow 1$ may be modest (Fig. 12). As the central T_i/T_e was varied from 1.9 to 1.5, the thermal confinement dropped by $<10\%$. Note that the impurity content [Fig. 12(c)] dropped below the nominal ITER value as density was increased, as is necessary to allow for dilution in burning plasma from helium ash. It appears that nominal ITER values of collisionality and $T_i/T_e = 1$ can be obtained in DIII-D with n/n_{GW} about 0.7. The main concern with increasing the density in DIII-D is altering the resistivity profile in such a way that q_{\min} drops below 1. However, this really is an accessibility issue for DIII-D rather than a fundamental physics issue.

Confinement scaling is essential for extrapolation of present conditions to estimate fusion gain in a burning plasma experiment. Several scalings to ITER-FEAT parameters have been tested in order to substantiate the claim that the present discharges represent a high gain solution. The technique used for the extrapolation is to take the experimental profiles and

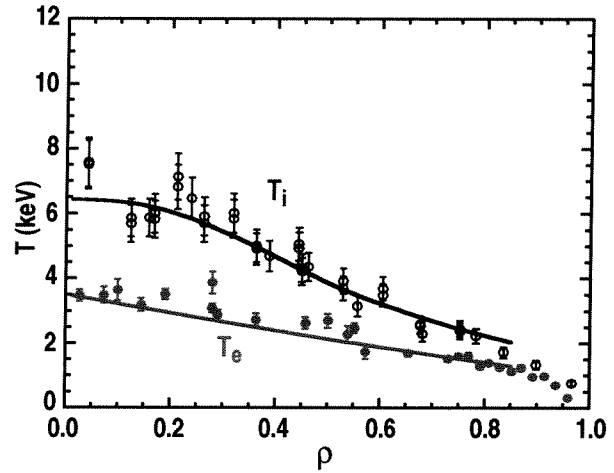


Fig. 11. Comparison of calculated (lines) and measured (points) electron (red) and ion temperatures (blue) for the long-pulse discharges shown in [11,12].

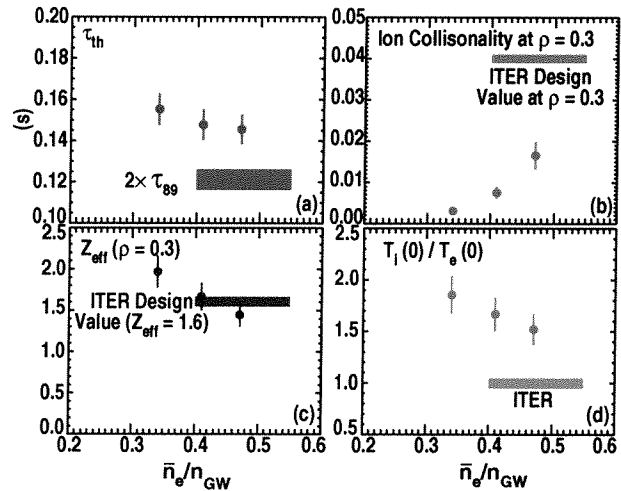


Fig. 12. Variation of (a) thermal energy confinement time (s), (b) ion collisionality at $\rho = 0.3$, (c) Z_{eff} at $\rho = 0.3$, and (d) $T_i(0)/T_e(0)$ versus density normalized to the Greenwald density. Nominal values for a $Q = 10$ scenario in ITER-FEAT are shown.

determine a multiplier for the confinement achieved compared to a scaling relation. Then the profiles are scaled to ITER size and field by maintaining the same β_N and confinement multiplier. The density is adjusted (downward) to remain at the Greenwald density limit. This reduction of collisionality will have only a modest effect since the scalings used have weak collisionality scaling. Since β and q are fixed, the extrapolation is dominated by the ρ_* scaling. For the burning plasma conditions, it is assumed that $T_i = T_e$. The electron temperature profile is used from the present experiment since it is assumed that heat conduction in the electron channel will likely dominate the power balance. Profiles from 5050 ms in the discharge shown in Fig. 1 were used for the calculations presented here.

Two types of ρ_* scaling are widely seen. First, a scaling $\chi \propto \chi_B \equiv eT/B$, known as Bohm scaling, is often seen in L-mode discharges. The ITER-89P scaling [5] for an early ITER global confinement database manifests a Bohm scaling. Projecting the discharge in Fig. 1 to ITER using a fixed $H_{89} = \tau_E/\tau_{89P}$ gives a fusion gain $Q = 7.6$. Raising β_N to 3.2 as shown in Figs. 7 and 8 raises Q to 12. Studies of ρ_* scaling in H mode indicate $\chi \propto \chi_B \rho_*$, known as gyroBohm scaling. This scaling is more optimistic for the increase in confinement with larger size and higher magnetic field. A gyroBohm, electrostatic model has been fit to the ITER H-mode global confinement database [21], with nearly the same error. Using this gyroBohm scaling, the lower β_N discharges will reach ignition even with a 20% reduction in the confinement multiplier. There are many caveats which must be attached to these projections such as the credibility of a peaked density profile in a burning plasma. However, this extrapolation exercise points to the huge benefit in fusion performance of high β_N . The fact that even a Bohm scaling allows $Q = 10$ solutions indicates that the present class of discharges warrants further study.

The ultimate limitation on pulse length at these parameters in DIII-D appears to be the maximum energy which the auxiliary heating systems can deliver. The neutral beam systems can deliver about 60 MJ for long pulse while the electron cyclotron (EC) and fast wave systems can deliver potentially around 10 MJ. The longest discharges now consume about 45 MJ at $\beta_N = 2.7$. At some point, the tile heating may present a problem; hence the testing of divertor sweeping as shown in Fig. 10. Tests of a radiative divertor with impurity seeding are planned. At present levels of steady performance, it should be possible to reach 10 s of high performance operation which would be $>3 \tau_R$. At higher β ($\beta_N = 3.2$), discharges longer than 5 s at high performance should be possible.

8. SUMMARY

A new stationary mode of operation has been discovered in DIII-D which has exciting prospects for high gain demonstrations in burning plasma experiments. The pressure profile is stationary for up to $36 \tau_E$ and the current profile is stationary to $>2 \tau_R$. This mode relies on active particle control rather than conditioning of the wall which can only manipulate the particle balance transiently. Stationary performance of $\beta_N = 2.7$, $\beta_{NH89} \sim 7$, and $\beta_{NH89}/q_{95}^2 = 0.39$ have been demonstrated. Discharges have been operated with $\beta_{NH89} \sim 9$ and $\beta_{NH89}/q_{95}^2 = 0.44$ for ~ 1 s near the estimated no-wall β limit. The key to accessing this high performance regime appears to be reaching high β before q_{min} reaches 1 and sawteeth begin. Under the influence of a small 3/2 tearing mode, the current profile relaxes to a stationary state with $q_{min} \geq 1$. Assuming a firm basis for extrapolating these discharges to a burning plasma experiment can be established, they represent an alternate scenario by which the high gain goals of a burning plasma experiment could be achieved with reduced potential for damage in a disruption. These discharges could also play a significant role in a technology testing phase where high gain at high duty cycle is important.

REFERENCES

- [1] ITER Physics Basis Editors, *et al.*, Nucl. Fusion **39**, 2137 (1999).
- [2] E. J. Strait, Phys. Plasmas **1**, 1415 (1994).
- [3] T. Dudok de Wit, *et al.*, Phys. Plasmas **1**, 3288 (1994).
- [4] R.J. La Haye, *et al.*, “Polarization Current and Neoclassical Tearing Mode Threshold in Tokamaks: Comparison of Experiment With Theory,” in Fusion Energy 2000, http://www.iaea.org/programmes/ripc/physics/fec2000/pdf/exp3_05.pdf
- [5] P.N. Yushmanov, *et al.*, Nucl. Fusion **30**, 1999 (1990)
- [6] R. Aymar, *et al.*, Plasma Phys. and Control. Fusion **44**, 519 (2002).
- [7] B.W. Rice, K.H. Burrell, L.L. Lao, Y.R. Lin-Liu, Phys. Rev. Lett. **79**, 2694 (1997).
- [8] D. Mikkelsen, Phys. Fluids B **1**, 333 (1989).
- [9] O. Sauter, *et al.*, Phys. Plasmas **6**, 7834 (1999).
- [10] C.B. Forest, *et al.*, Phys. Rev. Lett. **73**, 2444 (1994).
- [11] M.R. Wade, *et al.*, Phys. Plasmas **8**, 2208 (2001).
- [12] T.C. Luce, *et al.*, Nucl. Fusion **41**, 1585 (2001).
- [13] D.P. Brennan, *et al.*, Phys. Plasmas **9**, 2998 (2002).
- [14] R.J. La Haye, *et al.*, Nucl. Fusion **40**, 53 (2000).
- [15] R.J. La Haye, *et al.*, Phys. Plasmas **7**, 3349 (2000).
- [16] R. Maingi, *et al.*, Nucl. Fusion **36**, 245 (1996).
- [17] M.A. Mahdavi, *et al.*, J. Nucl. Mater. **290–293**, 950 (2001).
- [18] C.C. Petty, *et al.*, Nucl. Fusion **38**, 1183 (1998).
- [19] JET Team (presented by J.G. Cordey), Plasma Phys. and Control. Fusion Research 1996, Vol. 1 (International Atomic Energy Agency, Vienna, 1996) p. 603.
- [20] ITER H Mode Database Working Group, *et al.*, Nucl. Fusion **34**, 131 (1994).
- [21] C.C. Petty, *et al.*, Fusion Sci. Tech. **43**, 1 (2003).
- [22] Z. Chang, *et al.*, Nucl. Fusion **34**, 1309 (1994).
- [23] R.E. Waltz, *et al.*, Phys. Plasmas **5**, 1784 (1998).
- [24] C.C. Petty, *et al.*, Phys. Rev. Lett. **83**, 3661 (1999).

ACKNOWLEDGMENT

Work supported by the U.S. Department of Energy under Contracts DE-AC03-99ER54463, DE-AC05-00OR22725, W-7405-ENG-48, DE-AC04-94AL85000 and Grant DE-FG03-01ER54615.